**Proceedings of the ASME 2024
Internal Combustion Engine Division ICE Forward Conference
ICEF2024
October 20–23, 2024, San Antonio, TX**

ICEF2024-140006

A FUNDAMENTAL STUDY ON THE POTENTIAL LSPI PROMOTING MECHANISMS OF Ca AND Mg BASED OIL DETERGENTS

Matthew J. McAllister[1,2,†,*], Martin H. Davy[2,†], Luke J. Doherty[2], Laurent M. LePage[2], Christopher Wheeler[2],

[1]Caterpillar Inc., Peterborough, United Kingdom
[2]University of Oxford, Oxford, United Kingdom

ABSTRACT

Abnormal combustion, in its various forms, has presented a challenge to the design and operation of spark-ignited internal combustion engines for well over a century. During the last decade the relative prevalence of low speed pre-ignition (LSPI) in highly boosted and downsized engines has led to significant research efforts directed at understanding its origins. Two key mechanisms; oil droplet release from the piston top land crevice region and the accumulation and release of in-cylinder deposits, have both been shown to trigger LSPI. With respect to the oil release mechanism, multiple authors have reported a link between LSPI propensity and the calcium treat rate as detergent in the oil additive pack. It is, similarly, widely reported that magnesium based detergent packs do not promote LSPI in the same way. However, no fundamental explanation as to why calcium is 'bad' and why magnesium is 'good' has yet been presented in the literature. This paper reports the preliminary results from a series of fundamental shock tube experiments exploring the reactions between calcium and magnesium oxides, and a range of gases in relation to their potential as a trigger for LSPI. Visible light emissions are shown from shock heated calcium oxide particles in a 100% carbon dioxide environment at high temperature, T > 1173 K. Unexpectedly, light emitting reactions are also shown for calcium oxide in a 100% nitrogen environment at temperatures T > 773 K, suggesting that there may be a previously unidentified LSPI trigger mechanism in which nitrogen plays a key role. No visible emissions were seen from magnesium oxide powders.

Keywords: LSPI, Abnormal combustion. Oil additives, Calcium, Shock tube

NOMENCLATURE

Roman letters

CDST	Cold-Driven Shock Tube
ICE	Internal Combustion Engine
LSPI	Low Speed Pre-ignition
P	Pressure [MPa]
SI	Spark Ignition
T	Temperature [K]

Superscripts and subscripts

5	Test section value within test time

1. INTRODUCTION

Despite over a century of development, there remains more that can be done to improve the spark-ignited (SI) internal combustion engine (ICE). In recent times, three main factors have driven, and continue to drive, ICE development: (1) emissions legislation, (2) customer demand for increased specific performance, and (3) CO_2 reduction. Increasingly, vehicle manufacturers are employing highly boosted turbocharged 'downsized' engines to simultaneously reduce fuel consumption and increase specific performance [1–5]. However, the adoption of this new technology is challenged by, and has renewed interest in, an old problem. Abnormal combustion, in its various forms, has presented particular challenges to the design and operation of SI engines for well over a century. While the problem had largely been resolved for conventional naturally-aspirated and low-boost engines through improvements in combustion system design and fuel quality, it has been found that the combination of high brake mean effective pressure (BMEP) and low-speed, wide-open throttle operating conditions that can occur in these downsized engines can cause stochastic pre-ignition [6, 7].

The relative prevalence of low speed pre-ignition (LSPI) in this new generation of engines has led to significant research efforts directed at understanding its origins [8–12]. Two key mechanisms; oil droplet release from the piston top land crevice region and the accumulation and release of in-cylinder deposits, have both been shown to trigger LSPI [8, 13, 14]. Lubricating

---

†Joint first authors
*Corresponding author: matthew.mcallister@cat.com
Documentation for `asmeconf.cls`: Version 1.37, July 20, 2024.

oils require detergents to maintain the oil quality, to resist deposit formation and the acidification that results from exposure to combustion. Detergent components tend to be alkaline metals, typically present as a hydroxide or carbonate particles, which form a colloid with the base oil [15]. Calcium carbonate ($CaCO_3$) is one such detergent component that is commonly present in commercial lubricants [16]. However, despite its many advantages as an additive component, numerous researchers and research groups have demonstrated a clear link between the use of calcium in a lubricant's detergent pack and LSPI [17–19]. However, the precise mechanism by which calcium leads to increased LSPI tendency, as opposed to the observed behaviour of magnesium (Mg) based detergents for example [2, 18, 20], remains unknown. One potential mechanism, proposed by Moriyoshi and co-workers [21] and referred to hereinafter as the 'Chiba hypothesis', is as follows:

- Oil, containing calcium carbonate ($CaCO_3$) detergent, is ejected as a droplet or droplets from the oil film built up in the top land crevice region into the combustion chamber due to the piston motion
- The oil droplet or droplets are heated to in excess of 900 K during the combustion and exhaust processes and thermally decompose into calcium oxide (CaO) particles and carbon dioxide (CO_2). Some of the CaO particles are retained in the residual gas
- During the next compression stroke these retained particles are heated to in excess of 1000 K in the presence of CO_2 resulting in an exothermic carbonation reaction, Eq. (1), of sufficient energy as to trigger pre-ignition

$$CaO_{(s)} + CO_{2\,(g)} \longrightarrow CaCO_{3\,(s)} \quad \Delta H_{298K} = -178 \text{ kJ/mol} \quad (1)$$

A similar reversible carbonation reaction exists for magnesium carbonate. It too is exothermic, albeit to a lesser extent – Eq. (2)

$$MgO_{(s)} + CO_{2\,(g)} \longrightarrow MgCO_{3\,(s)} \quad \Delta H_{298K} = -118 \text{ kJ/mol} \quad (2)$$

Although Moriyoshi and co-workers successfully demonstrated the possibility of hot CaO particles triggering pre-ignition events in locally rich mixtures through numerical simulation [21], the Chiba hypothesis remains unproven in practice – not least due to the complexity of performing appropriately targetted experiments in the turbulent combustion environment of an ICE. The objective of the present experimental work was then to move the investigation of the Chiba hypothesis away from the ICE to a more closely controlled environment where it could be investigated at a more fundamental level. Accordingly, this paper will present the preliminary results of a fundamental study on the behaviour of metallic oil detergent derivatives, CaO and MgO, under controlled quiescent high temperature and pressure conditions provided by a reflected shock facility.

TABLE 1: CDST SPECIFICATIONS AND DESIGN CONDITIONS

Parameter	Value
Driver section i.d.	250 mm
Driven section i.d.	100 mm
Overall length	10.9 m
Design pressure (nominal)	6 MPa
Design temperture (nominal)	900 K
Maximum working pressure	15 MPa
Maximum working temperature	1500 k
Optical windows (4 orthogonal)	70 x 30 mm

2. MATERIALS AND METHODS

2.1 Experimental facility

The experiments reported in this work were performed on the University of Oxford Cold Driven Shock Tube (CDST). The CDST is a bespoke, reflected shock facility – equipped with an optically accessible working section – initially designed for characterisation of fuel sprays and the investigation of chemical kinetics under controlled engine-representative conditions of temperature and pressure. Full details of the facility's capabilities, design, optical access, instrumentation and operating characteristics are given in [22]. Table 1 summarizes the CDST's key specifications and nominal design conditions.

The basic principle of CDST operation is to generate a shock wave in the driven section of the tube using a relatively low cost, unheated (hence cold driven) high pressure driver gas, typically compressed air. The lower pressure (driven) gas is transiently shock heated to a higher pressure and temperature by the incident shock which, when correctly reflected from the end wall of the shock tube, brings the driven gas in the working section to rest, creating a quiescent high pressure and temperature 'slug' of the driven gas in which experiments can be performed. The temperature and pressure of the driven gas in the working section are then a function of the initial gas composition and the experimental setup. In this work, each 'condition' – driver and driven gas compositions and their respective initial pressures – required to produce the target conditions of temperature and pressure was calculated using the open-source quasi-one-dimensional gas dynamics code, L1d3 [23, 24].

The characteristic spatial and temporal development of the driven gas pressure is illustrated in Figs. 1 to 3, where Fig. 1 illustrates the initial state of the CDST prior to the diaphragm rupture, Fig. 2 the state of the driven gas prior to the incident shock reaching the end wall, and Fig. 3 the full spatio-temporal pressure development of the driver and driven gases. The numbered states in the figures are as follows: state (1) is the initial state of the driven gas, based on the L1d3 calculated initial conditions, state (4) describes the initial condition of the driver gas at the start of the experiment, state (3) is the result of the unsteady expansion of gas following the rupture of the diaphragm which causes gas to flow into the driven section, and state (2) is the result of the 'normal' shock-wave leaving the driver and following the gas flowing into the driven section, which compresses the upstream gas. Once the shock wave reaches the end of the driven section it is reflected. As the reflected shock moves in the

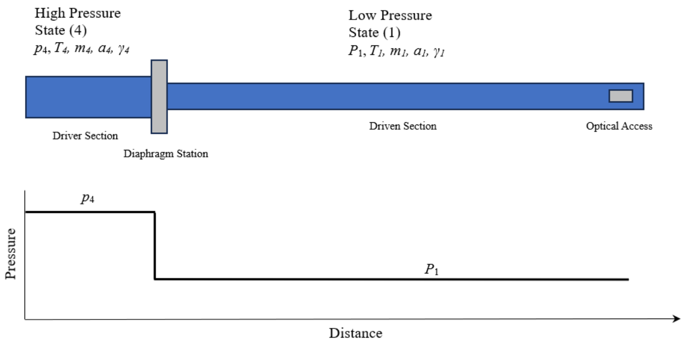

FIGURE 1: CDST INITIAL CONDITIONS, ADAPTED FROM [22]

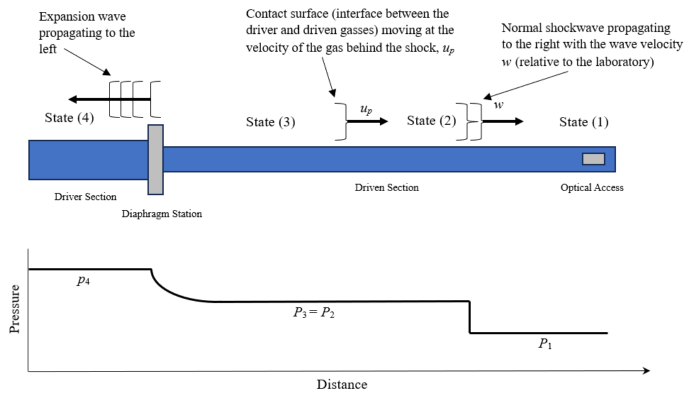

FIGURE 2: CDST CONDITIONS AT TIME, T , AFTER DIAPHRAGM RUPTURE, ADAPTED FROM [22]

direction of the driver, the gas behind the shock wave is brought to rest and further compressed to state (5), the desired test condition. Under nominal conditions the effective test time available in the facility is of the order of 3 ms.

Experimental runs are initiated by rupturing a pre-scored diaphragm or diaphragms initially separating the driver and driven gases. The CDST can be operated in either single or double diaphragm modes. In single diaphragm mode, rupture is achieved by increasing the pressure in the driver section until the diaphragm fails. In double diaphragm mode, two diaphragms, separated by an intermediate pressure are held until it is time to 'fire'. Thereafter, the intermediate pressure is removed, in-turn causing the first diaphragm, then the second diaphragm to rupture. The CDST is equipped with 11 high-frequency piezo-resistive pressure transducers (PCB 113 series ICP sensors) – flush mounted with the bore of the tube along the full length of the driven section – which record the generated shocks travelling down the tube and measure the pressure in the reflected shock region from which the bulk temperature can be inferred. The final three of these transducers – denoted STS (Shock Tube Station) 10, 11, and 12 respectively – are positioned within the optical test section, spaced 75 mm apart, with the final transducer at a nominal distance of 33 mm from the shock tube end wall. Figure 4 provides a cross-sectional view of the optical section and sensor placement. Two absolute pressure transducers (Kulite XTL-190LM) mounted into wall of the driver and shock tube are

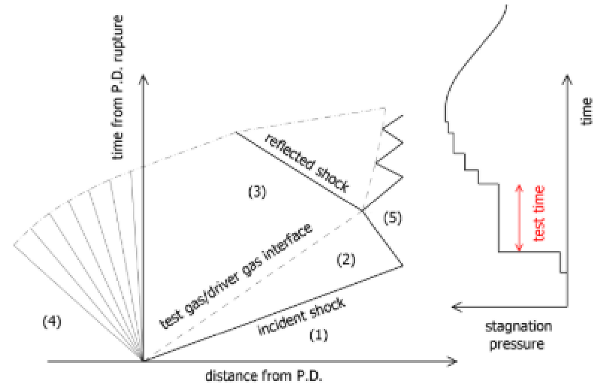

FIGURE 3: CDST X-T DIAGRAM, ADAPTED FROM [22]

used to monitor the driver and driven gas pressures during the filling process. The Kulite transducers are powered by a Fylde FE-379-TA modular amplifier, which also amplifies and conditions the signals prior to logging. Signals from the piezo-resitive sensors are recorded at a frequency of 2 MHz using a National Instruments data acquisition system controlled via the LabVIEW programming language program T4NIDAQ [25].

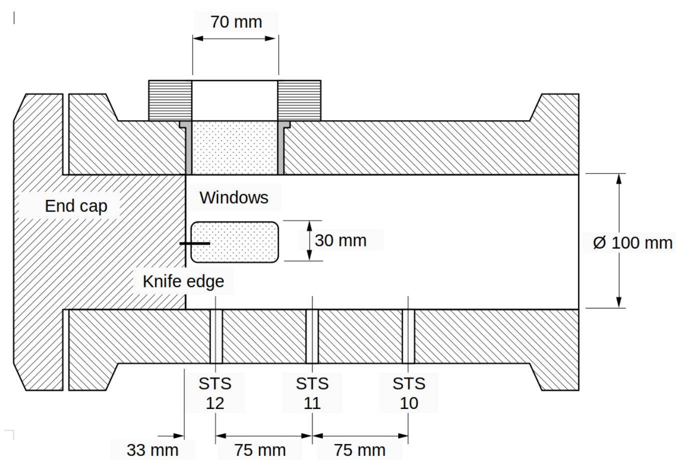

FIGURE 4: CROSS-SECTIONAL SCHEMATIC OF CDST OPTICAL SECTION (NOT TO SCALE). ALL IMAGES PRESENTED IN THE RESULTS SECTION HAVE BEEN CROPPED TO MATCH THE 70 MM X 30 MM WINDOW SIZE.

2.2 Methodology

As described in the introductory section, the aim of this present work was to study aspects of the LSPI promoting mechanism proposed in the 'Chiba hypothesis' under carefully controlled experimental conditions. This study then assumes that the first stage of the proposed mechanism, the thermal decomposition of the metal carbonates to oxide particles, has occurred. Moriyoshi reported visible light discharge from particles in the combustion chamber during LSPI [21], and bench-top experiments performed by the authors [26] confirmed a significant light emission when CaO powder was heated in a CO_2 environment. Accordingly, the metal oxide powders, CaO (Sigma

TABLE 2: EXPERIMENTAL TEST MATRIX (NOMINAL CONDITIONS)

Temperature [K]	Pressure [MPa]	Powder 0.20g ± 0.025g	Driven gases
773	1.90	CaO, MgO	CO_2, N_2
873	0.85	CaO	N_2
1058	0.62	CaO, MgO	CO_2, N_2, Ar
1173	0.97	CaO, MgO	CO_2

Aldrich ReagentPlus© 99.9%, trace metal basis and MgO (Sigma Aldrich ≥ 99.99%, trace metal basis) were dispersed and shock heated in various 100% gas environments within the CDST while the optical test was section monitored for visible light emissions through the quartz-windows. Table 2 details the matrix of tests performed.

The arrangements for powder dispersal within the CDST follows the work of Bayzn *et al.* [27] who used a simple knife-edge arrangement as a means of dispersing aluminium and nanocomposite thermite powders in a reflected shock tube as per Fig. 5. A similar plug/knife-edge arrangement was constructed and fitted to the optical section of the CDST. Approximately 0.20g of metal oxide powder was placed on the knife-edge at the start of each test. The CDST was cleaned of all residual powder and purged of gases using a vacuum pump between tests.

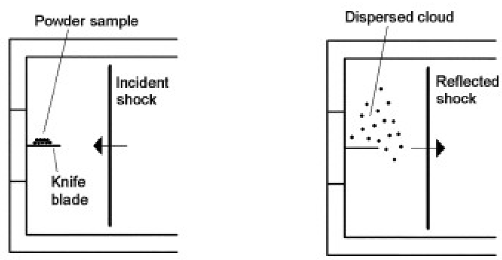

(a) Powder sample and incident shock

(b) Dispersed powder and reflected shock

FIGURE 5: KNIFE-EDGE METHOD FOR POWDER DISPERSAL IN THE CDST, MODIFIED FROM [27]

2.3 Optical systems

The optical section of the CDST was monitored for visible light emissions from the dispersed powder by means of a high speed video camera system and a photodiode (Thorlabs DET36A2). Data capture from the camera was triggered by the arrival of the incident shock at STS-9 (Shock Tube Station 9), the pressure transducer located immediately before the optical section of the facility. The results presented in this paper stem from three separate experimental campaigns performed on the CDST over a period of approximately 18 months. Two different camera systems were used in this time. Table 3 details the camera configurations (active sensor size and frame rates) used in each campaign.

TABLE 3: OPTICAL SYSTEMS

Campaign(s)	1	2 & 3
Camera	Photron FASTCAM Mini UX100	Photron FASTCAM Mini AX200
Sensor	1280 x 480	1024 x 672
Type	CMOS	CMOS
Pixel (μm)	10 x10	20 x 20
Range (ADC)	12-bit	12-bit
Speed (fps)	10,000	10,000
Lens	NIKKOR	Tamron

3. DATA POST-PROCESSING AND RESULTS

The data files collected by the DAQ contain temporal pressure information logged from each pressure sensor at known positions along the shock tube. The incident and reflected shock speeds were calculated by observing the pressure rise at different transducer locations. From this, the gas temperature in the working section of the CDST, T_5, was calculated by solving 1-D conservation equations for mass, momentum, and energy across the shock wave. The CDST was operated in both single and double diaphragm modes over the full course of the experimental study. Repeat tests under nominally identical operating conditions (driver and driven gas compositions, temperatures and pressures, targeting 1058 K and 0.62 MPa) were performed to establish the repeatability of the test temperatures. For single diaphragm operation (campaigns 1 & 2), the standard deviation on the mean $\sigma \approx 14$ K. When switched to double diaphragm operation in campaign 3 the uncertainty was reduced to $\sigma \approx 7$ K. This level of uncertainty is consistent with results from similar shock tube facilities published in the literature, e.g. [28]. The captured 12-bit high-speed camera data were saved as .mraw image sequences. Subsequently, representative individual images for display in this work were extracted from selected sequences and post-processed using Fiji (ImageJ) software [29]. The raw images were first cropped to the limits of the optical window and converted to 8-bit grey scale format prior to applying a conventional histogram normalisation method to enhance contrast.

Figure 6 shows the results of a preliminary test performed to confirm the efficacy of the powder dispersal via the knife blade method. As the incident shock arrives, the powder, simply illuminated here by an external light source, is seen to be pushed to the back of the knife blade, Fig. 6b. Subsequently, the reflected shock disperses the powder into the field of view, Fig. 6c and Fig. 6d. The powder is shown to be well dispersed in the CDST approximately 5 ms after the arrival of the incident shock at the timing point, Fig. 6d.

Initial experiments were performed with CaO powder in a 100% CO_2 environment in order to directly examine the carbonation reaction proposed by Moriyoshi [21]. Figure 7 shows a representative set of images taken from the nominal 1173 K, 0.97 MPa test condition (the temperature and pressures given in the figure caption detail the measured pressure and calculated temperature for the individual test shown). These images show a diffuse, but clearly visible, light emission from the reacting pow-

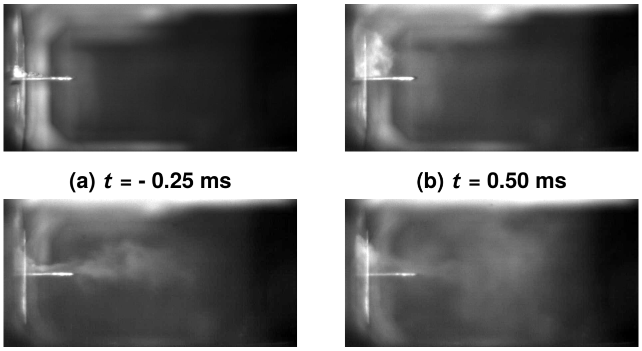

(a) t = - 0.25 ms (b) t = 0.50 ms (c) t = 3.00 ms (d) t = 5.00 ms

FIGURE 6: SHOCK INDUCED POWDER DISPERSAL, EXTERNAL ILLUMINATION OF WORKING SECTION, TEST #34, FRAME SPEED 4,00 FPS (ALL TIMES REFERENCED TO THE FIRST ARRIVAL OF SHOCK AT KNIFE EDGE)

der that is well dispersed across the majority of the field of view. It is notable that no visible light emission from the CaO powder in CO_2 environments was captured by either the high speed camera or photodiode at any of the lower test temperatures examined. It is also significant that no visible light emissions were seen from the MgO powder in CO_2 at any of the examined temperatures.

Figures 8 and 9 show the experimental results for CaO powder in an 100% N_2 environment at temperatures of 1158 K and 1058 K respectively. In these cases, rather unexpectedly, a vigorous reaction with a bright light emission is seen – so much so in fact that for the higher temperature case the CMOS camera images become saturated, see Fig. 8d. In the early stages of reaction the results from the higher temperature, 1158 K, case appear similar in nature to those seen for the CaO powder in CO_2 at the same test point, i.e. a relatively well distributed diffuse reaction, cf. Figs 7a - 7c and Figs. 8b - 8c – note here that both of these sets of images were collected during campaign 1 and were therefore captured using the same camera and lens set-up and settings. However in the latter stages of the visible light emission, the N_2 case images differ substantially from the CO_2 case in that there appears to be intense localised reactions, Figs 8e - 8h for example.

A similar trend of almost discrete particle-like behaviour is seen in the captured visible light emissions for the CaO powder in 100% N_2 at the temperature of 1058 K – Fig. 9. Note here that the images shown in this figure were captured in campaign 3 and that therefore the camera and lens set-ups and the image depth of field differs from the images shown in Fig. 7 and 8. While it may be that the camera/lens change have some influence over the comparative appearance of the visible reaction, it is nonetheless clear that there is still a strong, energetic, light emission from the CaO powder in N_2 at this temperature.

Figure 10 shows a series of representative images taken from the testing of CaO in a 100% N_2 environment at a target temperature of 873 K. In this case, the relatively low-intensity raw camera images have been further post-processed in order to highlight the behaviour that is clearly seen in the captured high-speed movie sequences. The images were first despeckled using median filter with a 3 x 3 kernel to remove noise, a Gaussian blur was then ap-

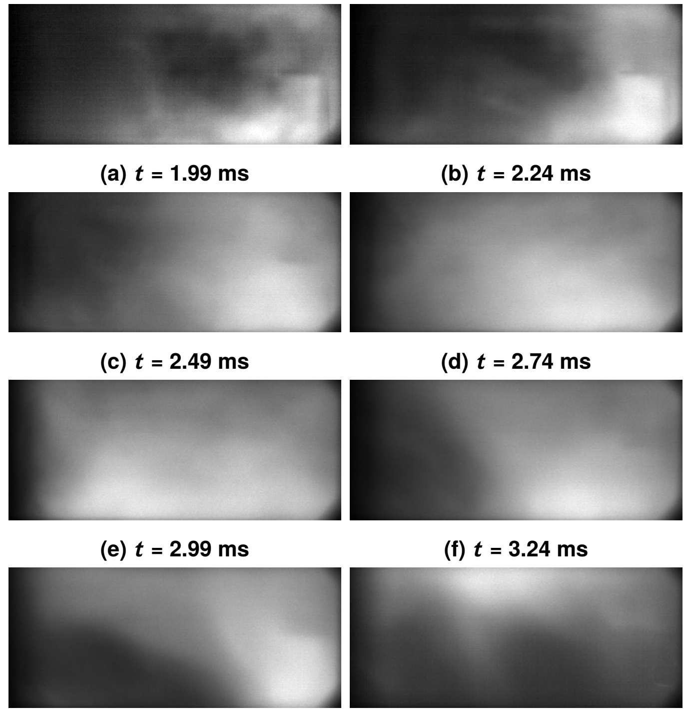

(a) t = 1.99 ms (b) t = 2.24 ms (c) t = 2.49 ms (d) t = 2.74 ms (e) t = 2.99 ms (f) t = 3.24 ms (g) t = 3.49 ms (h) t = 3.74 ms

FIGURE 7: REPRESENTATIVE HIGH SPEED IMAGES, CaO + CO_2, T_5 = 1185 K, P_5 = 0.98 MPa, CAMPAIGN 1, TEST #37, FRAME SPEED 4,000 FPS (ALL TIMES RELATIVE TO FIRST VISIBLE LIGHT EMISSION)

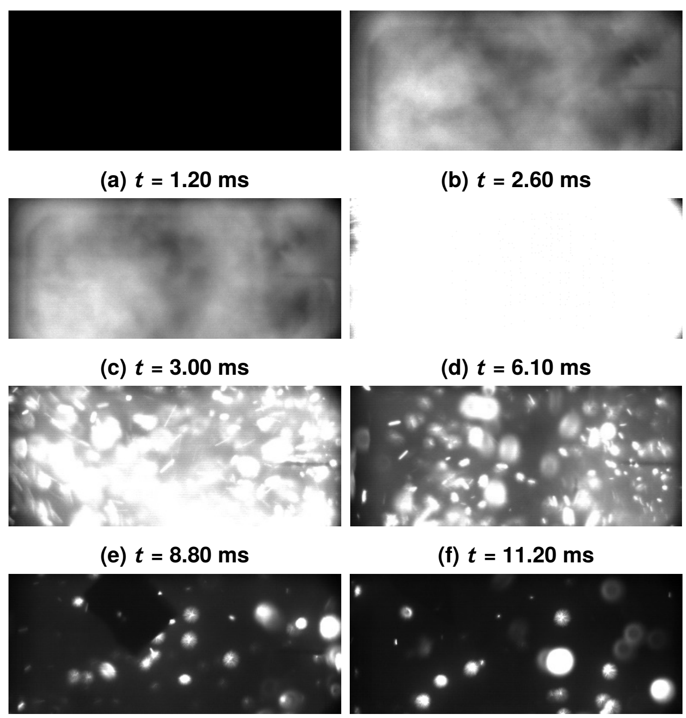

(a) t = 1.20 ms (b) t = 2.60 ms (c) t = 3.00 ms (d) t = 6.10 ms (e) t = 8.80 ms (f) t = 11.20 ms (g) t = 15.90 ms (h) t = 17.70 ms

FIGURE 8: REPRESENTATIVE HIGH SPEED IMAGES, CaO + N_2, T_5 = 1158 K, P_5 = 0.62 MPa, CAMPAIGN 1, TEST #39, FRAME SPEED 10,000 FPS (ALL TIMES RELATIVE TO FIRST VISIBLE LIGHT EMISSION)

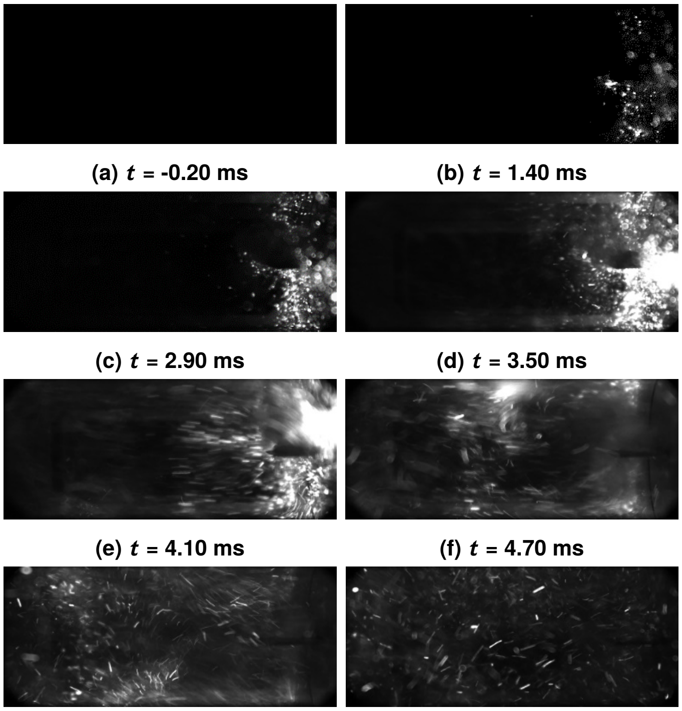

(a) t = -0.20 ms (b) t = 1.40 ms (c) t = 2.90 ms (d) t = 3.50 ms (e) t = 4.10 ms (f) t = 4.70 ms (g) t = 5.50 ms (h) t = 8.10 ms

FIGURE 9: REPRESENTATIVE HIGH SPEED IMAGES, CaO + N_2, T_5 = 1024 K, P_5 = 0.62 MPa, CAMPAIGN 3, TEST #145, FRAME SPEED 10,000 FPS (ALL TIMES RELATIVE TO FIRST VISIBLE LIGHT EMISSION)

plied to smooth the results, and finally the images' contrast was enhanced by stretching the histogram with a saturated pixel limit of 0.35%, thus the light intensity may not be directly compared with the intensity of reaction shown in previous figures. Nonetheless, the resulting images shown in Fig. 10 do fairly represent the behaviour of the CaO powder under these conditions. Visible reactions, albeit with low level light emissions, are seem to occur in small localized regions randomly distributed through the test section. The captured high-speed image sequences clearly show these light-emitting reaction zones being transported about the test section, thus confirming that despite their low intensity within the raw images they may not be discounted as either artefacts of the imaging or post-processing processes.

As noted in Table 2, tests were also performed with the CaO powder in N_2 at the lower temperature of 773 K. At this temperature, although the camera system did not capture any visible light emissions the photodiode data did suggest some low level emission. However, at the time of writing this particular result is still to be confirmed. No visible light emissions from the MgO powder in N_2 were recorded by either the imaging system or photodiode at any of the examined temperatures. Experiments were also performed with both CaO and MgO powders in a 100% argon environment at 1058 K. No light emissions were recorded in either case. Figure 11 presents a graphical summary of the experimental results.

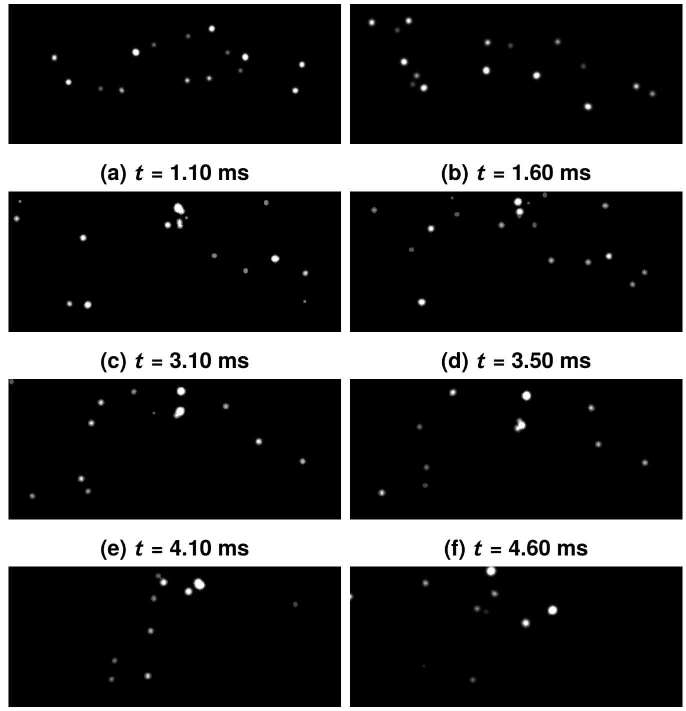

(a) t = 1.10 ms (b) t = 1.60 ms (c) t = 3.10 ms (d) t = 3.50 ms (e) t = 4.10 ms (f) t = 4.60 ms (g) t = 8.30 ms (h) t = 10.20 ms

FIGURE 10: REPRESENTATIVE HIGH SPEED IMAGES, CaO + N_2, T_5 = 869 K, P_5 = 0.85 MPa, CAMPAIGN 3, TEST #154, FRAME SPEED 10,000 FPS, (ALL TIMES RELATIVE TO FIRST VISIBLE LIGHT EMISSION)

4. DISCUSSION

This work set out to examine the hypothesis presented in [21] that the carbonation reaction between calcium oxide particles and carbon dioxide, Eq.(1), could act as a trigger for LSPI in spark-ignited engines. However, the results presented herein neither unambiguously prove nor disprove the hypothesis. A visible light emission, attributed by the authors to this carbonation reaction is shown – Fig.7 – at a nominal test temperature of 1173 K. However, no visible light emissions for CaO powder in 100% CO_2 environments were detected at any of the lower temperatures examined. Moreover, the light emissions from CaO at the nominal 1173 K test point were inconsistent. Of five repeat tests at this test point, light emission was recorded in three cases. On closer inspection of the test data, the two non-emitting test points correspond to the two lowest calculated true test temperatures, 1164 and 1182 K respectively, while the three emitting case temperatures range from 1185 to 1192 K.

The inconsistent nature of the CaO + CO_2 carbonation reaction perhaps suggests that these experimental conditions may lie close to a threshold temperature level for the reaction. With respect to the potential of the carbonation reaction as a trigger for LSPI, the temperature required to stimulate a visible reaction in the experiments reported herein – approximately 1185 K – is considerably in excess of the typical in-cylinder bulk gas temperature found in an SI engine during typical LSPI prone operating conditions – expected to be in the region of 600 - 720 K depending on combustion system. This of course does not preclude the reac-

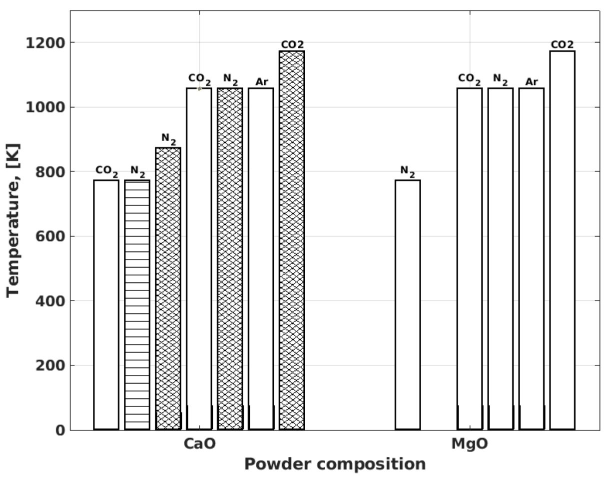

FIGURE 11: SUMMARY OF EXPERIMENTAL RESULTS (CROSS-HATCHED BARS INDICATE LIGHT EMISSION, HORIZONTAL HATCHING IMPLIES UNCONFIRMED LIGHT EMISSION, NO HATCHING INDICATES NO LIGHT EMISSION)

tion being triggered in an engine by localised hot-spots of residual CO_2. It is also potentially significant that the numerical simulations of Moriyoshi and co-workers identified a dependency on particle size [21] which was not investigated in the current work.

While the results of the present study do not rule out the CaO + CO_2 carbonation reaction as a potential trigger for LSPI, the unexpected, vigorous, reaction of the CaO powder when shock heated in a N_2 environment does suggest the existence of an, as yet unidentified, alternative reaction pathway for CaO to trigger LSPI in which nitrogen play a key role. In contrast to the CaO + CO_2 results, visible reactions were detected with CaO + N_2 at significantly lower temperatures. Moreover, these results were highly repeatable with visible emissions occurring in every CaO + N_2 test case examined over all three test campaigns where the temperature was in excess of 773 K. That nitrogen is key to this potential new pathway is confirmed by the absence of reaction where the nitrogen was replaced by argon.

The results do show some potentially significant differences between the visible light emissions that are captured from the CO_2 and N_2 cases. The relatively diffuse, in the case of CO_2, and intense discrete particle like, in the case of the N_2, appearance of the images has already been mentioned. The duration of light emission also differs substantially in each case. In the CaO + CO_2 case, Fig. 7, the total duration of light emission is less than 2 ms (the next image in the sequence shown is dark). For the CaO + N_2 cases, Figs. 8, 9, and 10, detectable light emissions occur over periods of approximately 47, 54, and 70 ms respectively, i.e. both increasing with decreasing temperature and for a substantially longer duration than the CO_2 case and also, perhaps significantly, for a period that is substantially longer than the nominal test time of the shock tube facility.

The maximum test time of a shock tube, the period during which the driven gas exists as a nominally quiescent slug at the designed test temperature and pressure following the passing of the reflected shock, is provided by careful tailoring of the gas interface (contact surface) condition. The CDST does not provide perfectly tailored conditions in the present experiments, as a result, the temperature in the optical section may, in the case of over-tailoring, further increase following the nominal test time with the interface between the driver and driven gases – in this case air – moving further into the working section [30, 31]. Alternatively, where conditions are under-tailored, the temperature in working section will be decreased after the nominal test time. In both cases, the available test time will be reduced from the theoretical maximum - often substantially. Figure 12 shows an example pressure trace from sensor STS-12 positioned in the optical section of the CDST for an over-tailored condition.

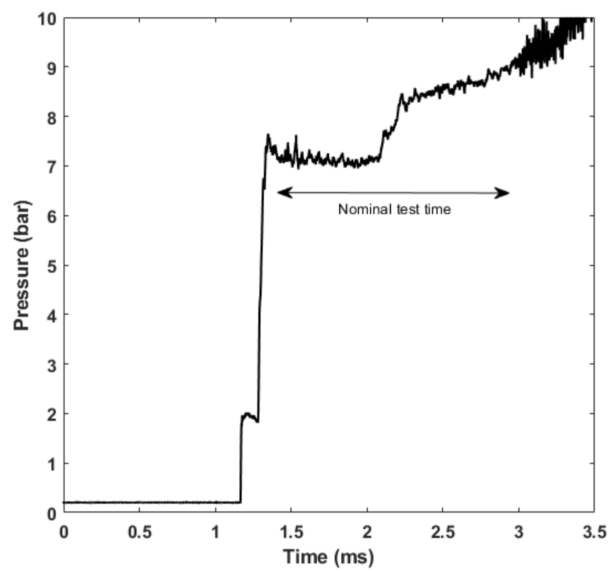

FIGURE 12: STS-12 PRESSURE TRACE, TEST #145, CaO + N_2, T_5 = 1024 K, P_5 = 0.62 MPa, CAMPAIGN 3

The figure shows a relatively short test time at the design conditions. Approximately half way through the test time there was a small rise in pressure, consistent with other similar tests, but not present when there was no powder on the knife blade. Thereafter, the main rise in pressure in the test section (where there is expected to be a corresponding rise in temperature in the test section gases as illustrated by the simulations of Coombs and Akih-Kumgeh [31]). These effects and their potential influence on the interpretation of the results of this study are currently marked for further investigation. Similarly, the potential effects of non-ideal flow behaviour in the working section, such as shock bifurcation caused by the interaction of the reflected shock with the boundary layer generated by the incident shock [32] will be considered in future work.

5. CONCLUSIONS

This work presents preliminary results from a fundamental shock tube study into potential LSPI promoting mechanisms of Ca and Mg based oil detergents, specifically potential reactions between CaO and MgO powders and two gases that are commonly found in-cylinder, CO_2 and N_2. The results are consistent with the strong body of evidence in the literature indicating that calcium-based detergents may act as potential triggers for LSPI whereas Mg based detergents do not. No detectable light emissions were noted from the MgO powder under any of the examined gas/temperature combinations considered in this study.

Light emission attributed to the exothermic carbonation reaction, Eq.(1), proposed as a potential LSPI trigger by Moriyoshi *et al.* [21], was observed at a temperature of 1185 K in a 100% CO_2 environment. No detectable light emissions were found for this powder/gas combination at lower temperatures. The in-cylinder bulk gas temperature at the inception of LSPI is expected to be below 1185 K, nevertheless, the possible presence of hot residual gas pockets within the cylinder, and the particle size effects noted by Moriyoshi, lead the authors to conclude that the 'Chiba hypothesis' and the reactions described therein remain a plausible trigger mechanism for LSPI.

A strong light emitting reaction was unexpectedly observed when the CaO powder was shock heated in a 100% N_2 environment. These light emissions were found at all temperatures examined above 773 K, i.e. at significantly lower temperatures than for the CaO + CO_2 case. The precise reaction mechanism or pathway by which these light emissions are generated has not been identified in this work and remains the subject of further investigation. Nonetheless, the results of this study strongly suggest the existence of a potential LSPI trigger mechanism from Ca based detergent packs in which nitrogen plays a key role.

ACKNOWLEDGMENTS

The authors wish to gratefully acknowledge the significant role played by Dr Rowland Penty Geraets in the design and commissioning of the experiments and for his contributions to the data collection during Campaign 1. The financial contributions of BP Lubricants UK and the Advanced Propulsion Centre UK (APC) through an APC 'Developing internal combustion engines of the future' scheme grant are gratefully acknowledged also. For the purpose of Open Access, the author has applied a CC BY public copyright licence to any Author Accepted Manuscript (AAM) version arising from this submission. The authors would also like to thank the Dept. of Engineering Science technicians and maintenance teams in the Osney Thermofluids Institute (OTI) for facilities support.

REFERENCES

[1] Miller, James, Taylor, James, Freeland, P., Warth, M., Dingelstadt, R. and Mueller, R. "Future Gasoline Engine Technology and the Effect on Thermal Management and Real World Fuel Consumption." (2013)DOI 10.4271/2013-01-0271. URL https://www.semanticscholar.org/paper/4ab71d890ddb8ac2a1c53603a297792ef2e7fad3.

[2] Leach, B., Pearson, R., Ali, R. and Williams, John A. "CO 2 Emission Reduction Synergies of Advanced Engine Design and Fuel Octane Number." (2014)DOI 10.4271/2014-01-2610. URL https://www.semanticscholar.org/paper/eee0ceca8dc23a15ff7eb9be999ecea1c10ef599.

[3] Turner, J., Popplewell, A., Richardson, S., Lewis, A., Akehurst, S., Brace, C. and Bredda, S. "Ultra boost for economy: realizing a 60% downsized engine concept." (2013)DOI 10.1533/9781782421849.1.3. URL https://www.semanticscholar.org/paper/7831e71c068a557592ba81f4b42e340e9d02c1a8.

[4] Elmagdoub, Abdelrahman W. M., Carlson, Urban, Halmearo, Mattias, Turner, J., Brace, C., Akehurst, S. and Zhang, Nic. "Freevalve: Control and Optimization of Fully Variable Valvetrain-Enabled Combustion Strategies for Steady-State Part Load Performance and Transient Rise Times." (2023)DOI 10.4271/2023-01-0294. URL https://www.semanticscholar.org/paper/06dd37a0cf9d057ea20f2bdcccc8d7b215805d87.

[5] Leach, F., Stone, R., Richardson, D., Lewis, A., Akehurst, S., Turner, J., Remmert, S., Campbell, S. and Cracknell, R. "Particulate emissions from a highly boosted gasoline direct injection engine." (2018)DOI 10.1177/1468087417710583. URL https://www.semanticscholar.org/paper/f751444f103963b33689a5eb96638384d2e16dca.

[6] Rönn, Kristian, Swarts, Andre, Kalaskar, Vickey, Alger, Terry, Tripathi, Rupali, Keskiväli, Juha, Kaario, Ossi, Santasalo-Aarnio, Annukka, Reitz, Rolf and Larmi, Martti. "Low-speed pre-ignition and super-knock in boosted spark-ignition engines: A review." *Progress in Energy and Combustion Science* Vol. 95 (2023): p. 101064. DOI 10.1016/j.pecs.2022.101064.

[7] Jatana, Gurneesh S., Splitter, Derek A., Kaul, Brian and Szybist, James P. "Fuel property effects on low-speed pre-ignition." *Fuel* Vol. 230 (2018): pp. 474–482. DOI 10.1016/j.fuel.2018.05.060.

[8] Okada, Yoshihiro, Miyashita, Shigeki, Izumi, Yoshihiro and Hayakawa, Yutaka. "Study of Low-Speed Pre-Ignition in Boosted Spark Ignition Engine." *SAE International Journal of Engines* Vol. 7 No. 2 (2014): pp. 584–594. DOI 10.4271/2014-01-1218.

[9] Chapman, Elana M. and Costanzo, Vincent S. "A Literature Review of Abnormal Ignition by Fuel and Lubricant Derivatives." *SAE International Journal of Engines* Vol. 9 No. 1 (2015): pp. 107–142. DOI 10.4271/2015-01-1869.

[10] Kuboyama, Tatsuya, Moriyoshi, Yasuo and Morikawa, Koji. "Visualization and Analysis of LSPI Mechanism Caused by Oil Droplet, Particle and Deposit in Highly Boosted SI Combustion in Low Speed Range." *SAE International Journal of Engines* Vol. 8 No. 2 (2015): pp. 529–537. DOI 10.4271/2015-01-0761.

[11] Morikawa, Koji, Moriyoshi, Yasuo, Kuboyama, Tatsuya, Imai, Yasuo, Yamada, Toshio and Hatamura, Koichi. "Investigation and Improvement of LSPI Phenomena and Study of Combustion Strategy in Highly Boosted SI Combustion in Low Speed Range." *SAE Technical Paper Series* No. 2015-01-0756 (2015). DOI 10.4271/2015-01-0756.

[12] Splitter, Derek, Kaul, Brian, Szybist, James, Speed, Lake, Zigler, Bradley and Luecke, Jon. "Fuel-Lubricant Interactions on the Propensity for Stochastic Pre-Ignition." *SAE Technical Paper Series* Vol. 2019-24-0103 (2019). DOI 10.4271/2019-24-0103.

[13] Dahnz, C., Han, Kyung-Man, Spicher, U., Magar, M., Schießl, R. and Maas, U. "Investi-

gations on Pre-Ignition in Highly Supercharged SI Engines." (2010)DOI 10.4271/2010-01-0355. URL https://www.semanticscholar.org/paper/3a7fa1aa1ddb651725ecbc0bedbef9699f1a7746.

[14] Shimizu, Kento, Takahata, Shuhei, Miura, Kenta, Shoji, Hideo, Iijima, Akira, Utaka, Toshimasa and Tamura, Kazushi. "Influence of Calcium-Based Additives with Different Properties on Abnormal Combustion in an SI Engine." *SAE Technical Paper Series* Vol. 2016-11-08 (2016). DOI 10.4271/2016-32-0007.

[15] Seddon, E.J., Friend, C.L. and Roski, J.P. *Detergents and Dispersants*. Springer Netherlands, Dordrecht (2010): pp. 213–236. DOI 10.1023/b105569_7. URL https://doi.org/10.1023/b105569_7.

[16] Tang, Hong-Zhi and Jao, Tze-Chi. *Detergents*. Springer US, Boston, MA (2013): pp. 720–726. DOI 10.1007/978-0-387-92897-5_922. URL https://doi.org/10.1007/978-0-387-92897-5_922.

[17] Miyasaka, Tomomi, Miura, Kenta, Hayakawa, Norikuni, Ishino, Takashi, Iijima, Akira, Shoji, Hideo, Tamura, Kazushi, Utaka, Toshimasa and Kamano, Hideki. "A Study on the Effect of a Calcium-Based Engine Oil Additive on Abnormal SI Engine Combustion." *SAE International Journal of Engines* Vol. 8 No. 1 (2015): pp. 206–213. DOI 10.4271/2014-32-0092.

[18] Miura, Kenta, Shimizu, Kento, Hayakawa, Norikuni, Miyasaka, Tomomi, Iijima, Akira, Shoji, Hideo, Utaka, Toshimasa, Tamura, Kazushi and Kamano, Hideki. "Influence of Ca-, Mg- and Na-Based Engine Oil Additives on Abnormal Combustion in a Spark-Ignition Engine." *SAE International Journal of Engines* Vol. 9 No. 1 (2016): pp. 452–457. DOI 10.4271/2015-32-0771.

[19] Spicher, Ulrich, Gohl, Marcus, Magar, Max and Hadler, Jens. "The Role of Engine Oil in Low-speed Pre-ignition." *MTZ worldwide* Vol. 77 No. 1 (2016): pp. 60–63. DOI 10.1007/s38313-015-0079-6.

[20] Fletcher, Kristin A., Dingwell, Lisa, Yang, Kongsheng, Lam, William Y. and Styer, Jeremy P. "Engine Oil Additive Impacts on Low Speed Pre-Ignition." *SAE International Journal of Fuels and Lubricants* Vol. 9 No. 3 (2016): pp. 612–620. DOI 10.4271/2016-01-2277.

[21] Moriyoshi, Y., Yamada, Toshio, Tsunoda, Dai, Xie, Mingzhao, Kuboyama, Tatsuya and Morikawa, K. "Numerical Simulation to Understand the Cause and Sequence of LSPI Phenomena and Suggestion of CaO Mechanism in Highly Boosted SI Combustion in Low Speed Range." (2015)DOI 10.4271/2015-01-0755. URL https://www.semanticscholar.org/paper/7167d514164a61b3894b041f125441c45723f6af.

[22] Camm, J., Davy, M., Fang, Xiaohan, Doherty, L., McGilvray, M. and Foerster, F. "The Oxford Cold Driven Shock Tube (CDST) for Fuel Spray and Chemical Kinetics Research." (2018)DOI 10.4271/2018-01-0222. URL https://www.semanticscholar.org/paper/7e431cbd524352eb5db85d67069a4663db3bdbc8.

[23] Jacobs, P. "Shock Tube Modelling With L1d." (1998)URL https://www.semanticscholar.org/paper/cafec71bded2304d6cdd37863389efb6504c7b93.

[24] Jacobs, P. "L1d: A Computer Program for the Simulation of Transient-Flow Facilities." (1999)URL https://www.semanticscholar.org/paper/bd1a707cc35997687e2610f5ca8a8df7e8823d63.

[25] Ridings, A. "UQ's T4 Shock Tunnel Data Acquisition System." *2012 National Instruments Technical Symposium, Brisbane, QLD, Australia*. 2012.

[26] McAllister, Matthew J. "Insights into Abnormal Combustion in Advanced Gasoline Engines." Ph.D. Thesis, Department of Engineering Science. 2025.

[27] Bazyn, T., Glumac, N., Krier, H., Ward, T. S., Schoenitz, M. and Dreizin, E. "REFLECTED SHOCK IGNITION AND COMBUSTION OF ALUMINUM AND NANOCOMPOSITE THERMITE POWDERS." (2007)DOI 10.1080/00102200600637261. URL https://www.semanticscholar.org/paper/af33ab4b0c6bbbd1165ca0c96f5d371d11beb834.

[28] Wu, N., Bushe, W. K. and Davy, M. H. "On the experimental validation of combustion simulations in turbulent non-premixed jets." *Combustion Theory and Modelling* Vol. 14 No. 6 (2010): pp. 855–874. DOI 10.1080/13647830.2010.517274.

[29] Schindelin, J., Arganda-Carreras, Ignacio, Frise, E., Kaynig, V., Longair, M., Pietzsch, T., Preibisch, S., Rueden, C., Saalfeld, S., Schmid, Benjamin, Tinevez, J., White, D. J., Hartenstein, V., Eliceiri, K., Tomančák, P. and Cardona, A. "Fiji: an open-source platform for biological-image analysis." (2012)DOI 10.1038/nmeth.2019. URL https://www.semanticscholar.org/paper/d018241fe067d7bd54165e3c6d34e248a55437df.

[30] Huang, Jian. "Experimental shock tube study of ignition promotion for methane under engine relevant conditions." (2001)DOI 10.14288/1.0080948. URL https://www.semanticscholar.org/paper/d6f12f70923d07cee0c81407097cd7b3ab44588f.

[31] Coombs, D. and Akih-Kumgeh, B. "Numerical investigation of the impact of tailored driver gases and driver inserts on shock tube flows." *Shock Waves* Vol. 28 No. 5 (2018): pp. 1097–1107. DOI 10.1007/s00193-018-0851-z.

[32] Kleine, H., Lyakhov, V. N., Gvozdeva, L. G. and Grönig, H. "Bifurcation of a reflected shock wave in a shock tube." (1992). DOI 10.1007/978-3-642-77648-9_36.

[33] Wang, Zhi, Liu, Hui and Reitz, Rolf D. "Knocking combustion in spark-ignition engines." *Progress in Energy and Combustion Science* Vol. 61 (2017): pp. 78–112. DOI 10.1016/j.pecs.2017.03.004.

[34] Hayakawa, Norikuni, Miura, Kenta, Miyasaka, Tomomi, Ishino, Takashi, Iijima, Akira, Shoji, Hideo, Tamura, Kazushi, Utaka, Toshimasa and Kamano, Hideki. "A Study on the Effect of Zn- and Mo-Based Engine Oil Additives on Abnormal SI Engine Combustion using In-Cylinder Combustion Visualization." *SAE International Journal of Engines* Vol. 8 No. 1 : pp. 214–220. DOI 10.4271/2014-32-0096.

[35] Tamura, Kazushi, Utaka, Toshimasa, Kamano, Hideki, Hayakawa, Norikuni, Miyasaka, Tomomi, Ishino, Takashi, Iijima, Akira and Shoji, Hideo. "Abnormal Combustion Induced by Combustion Chamber Deposits Derived from Engine Oil Additives in a Spark-Ignited Engine." *SAE International Journal of Engines* Vol. 8 No. 1 : pp. 200–205. DOI 10.4271/2014-32-0091.

[36] Welling, Orian, Moss, James, Williams, John and Collings, Nick. "Measuring the Impact of Engine Oils and Fuels on Low-Speed Pre-Ignition in Downsized Engines." *SAE International Journal of Fuels and Lubricants* Vol. 7 No. 1 (2014): pp. 1–8. DOI 10.4271/2014-01-1219.